Springer

KSME

Journal of Mechanical Science and Technology 26 (8) (2012) 2439~2449
www.springerlink.com/content/1738-494x
DOI 10.1007/s12206-012-0622-1

Dynamics of universal joints, its failures and some propositions for practically improving its performance and life expectancy †

Farzad Vesali, Mohammad Ali Rezvani* and Mohammad Kashfi

School of Railway Engineering, Iran University of Science and Technology, Tehran, 16845-13114, Iran

(Manuscript Received July 11, 2011; Revised February 25, 2012; Accepted March 13, 2012)

Abstract

A universal joint also known as universal coupling, U joint, Cardan joint, Hardy-Spicer joint, or Hooke's joint is a joint or coupling in a rigid rod that allows the rod to 'bend' in any direction, and is commonly used in shafts that transmit rotary motion. It consists of a pair of hinges located close together, oriented at 90° to each other, connected by a cross shaft. The Cardan joint suffers from one major problem: even when the input drive shaft rotates at a constant speed, the output drive shaft rotates at a variable speed, thus causing vibration and wear. The variation in the speed of the driven shaft depends on the configuration of the joint. Such configuration can be specified by three variables. The universal (Cardan) joints are associated with power transmission systems. They are commonly used when there needs to be angular deviations in the rotating shafts. It is the purpose of this research to study the dynamics of the universal joints and to propose some practical methods for improving their performance. The task is performed by initially deriving the motion equations associated to the universal joints. That is followed by elaborating on the oscillatory behavior in the rotational speed and the torque that transmits through the intermediary shaft. The forces in the joint bearings are calculated by using an analytical method that is also supported by the numerical modeling. Such models are also used in order to calculate the rhythm and the amount of the excess loads on the joint. This is suggested as a systematic procedure in the search for the causes of the failures in these popular bearings. With the same purpose in mind some defected bearings with deformed sections were selected for the laboratory examinations. By analyzing the loading behavior and the surface conditions of the defected bearings and by comparison with the known fatigue theories attempts are made in order to dig into the causes for the failures in these joints and their bearing surfaces. With the aim of improving the performance and the life expectancy of these popular elements of the machineries, some practical recommendations are also suggested.

Keywords: Machinery failure; Bearing failure; Failure analysis; Fatigue failure; Solidworks modeling

1. Introduction

The idea of a mechanism that can provide slight inclination to the direction of the rotating shafts has long been thought of by the engineers. Artobolevsky introduced a handful of such mechanisms in his book [1]. Some of such mechanisms with their corresponding characteristic curves are presented in Fig. 1.

Failure of the universal joints can end up with serious consequences and it can be very costly. It causes sudden disruptor in the supply of power between its source and the consumer device. Therefore, many studies are performed in order to recognize the nature of the corresponding forces and the failure within these mechanisms. For example, Hajirezaei & Ahmadi have reported their research results on the effect of cracks in fragile failure of Cardan joints [2]. Bayrakceken, et al. reported research results on two cases of failure in the power transmission system on vehicles equipped with the universal joints [3]. All such studies concentrated on the failure in the universal joints or its connecting rods, in a general sense. There is hardly any research report specifically concerned with the failure of the bearings in the universal joints. However, in practice there have been many cases of failure associated with the malfunctioning universal joint bearings.

2. The universal joint mechanism

In 1904, Clarence Spicer, a young engineering graduate from Cornell University, registered his invention of a mechanism [4]. Since then, the mechanism that was called the Cardan joint has found widespread industrial applications. The Cardan joint is amongst the most popular universal joints. It is widely used in the mechanical couplings and joints with the pre-condition that the input drive shaft and the output drive shaft are not aligned. It may also be desired to permit some angular deviations along the axis of rotation, Fig. 2.

The Cardan joint comprises of the three main parts includ-

*Corresponding author. Tel.: +98 21 77491029, Fax.: +98 21 77451568
E-mail address: rezvani_ma@iust.ac.ir
† Recommended by Editor Yeong June Kang

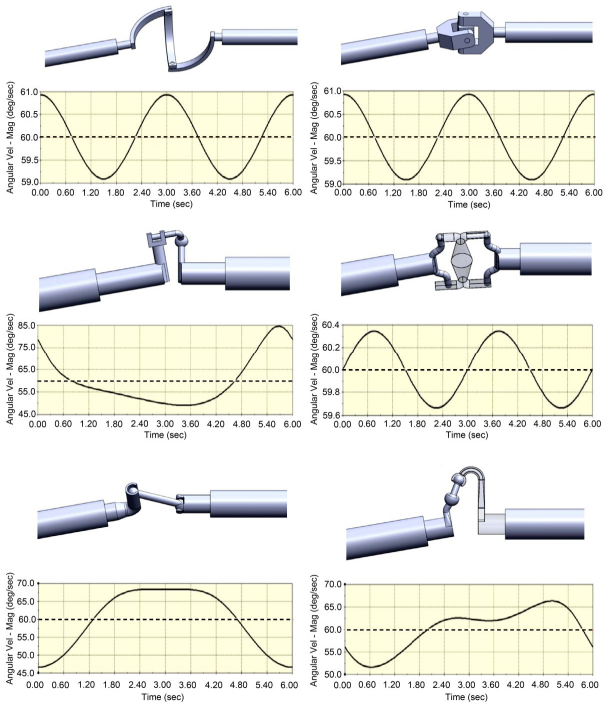

Fig. 1. Samples of the universal joints and the corresponding characteristic curves that were introduced by Artobolevsky, the dashed lines indicate angular velocity of the input drive shaft and the heavy lines indicate angular velocity of the output drive shaft [1].

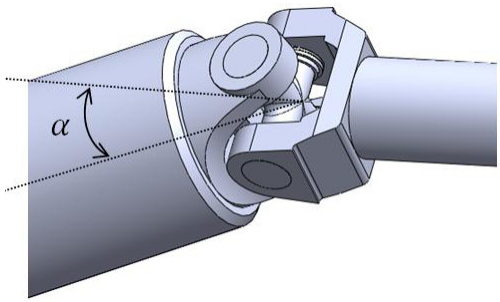

Fig. 2. Schematic of the Cardan joint.

ing the input drive shaft, the output drive shaft and the cross like piece. Two points of the cross piece connect to the input drive shaft and two other points connect to the output drive shaft. Connections are provided by the needle bearings.

It is an important aspect of these bearings that while in action they never go through complete cycles. In other words, each of these bearings revolves only a few degrees around its axis before returning to its original position. Therefore, there are only a group of balls in these bearings that take the bearing load. On the other hand, even if the angular speed of the input drive shaft is constant, the angular speed of the output drive shaft oscillates. The size of such oscillation depends on the amount of the angular deviation of the output drive shaft.

These couplings are widely used in the automobile power transmission systems. However, they are prone to wear and malfunction and need to be replaced in comparatively short intervals of time. Naturally, it means that such parts have limited life span.

2.1 Research background

Numerous mechanisms are used to transmit power between traversing shafts. Amongst them Hooke's joints are the most commonly used [5]. Hooke's joint is categorized as the Cardan joint and the spherical joint. These joints have relative intersecting angles of 15 and 45 degrees, respectively. These types of joints are used in the equipments that are capable of high power transmission. However, the angular velocity of the driven shaft is not constant. This means that the ratio of the output velocity to the input velocity is not the same at all angular positions [6].

Bayrakceken, et al. [3] carried out the fracture analysis of a universal joint yoke and a drive shaft of an automobile power transmission system. They concluded that crack propagation resulted from highly stressed points and fatigue failures are the main reasons behind the universal joints' failures. They also concluded that some modification on the design of the joint may be considered, in order to prevent such failures. The mild stress concentration also speeds up the failure.

Power transmission system of vehicles consists of several components that frequently encounter unfortunate failures. Heyes [7] studied the common failure types in automobiles. He revealed that failures in the transmission system cover quarter of all the failures in the automobiles. Some common reasons for such failures are the manufacturing and the design shortcomings. The poor maintenance, the faulty material as well as the mishandling by the users are also the contributing factors.

There are also reports by some researchers on the failure of the power transmission systems [8-11]. Bayrakceken analyzed the failure of a pinion shaft of a differential [12]. Kepceler, et al. studied the stress and life calculation of the elements of the power transmission system of a four wheel drive vehicle [13]. Hummel and Chassapis [14] researched on the design of the universal joints. They came up with some suggestions on the configuration design and optimization of the universal joints with manufacturing tolerances. They also developed a systematic approach to the design and optimization of the ideal universal joint [15]. The principals to design universal joints with the minimum diameter required to handle a given input torque for a given joint angle was derived.

In earlier designs, the front-wheel-drive automobile that was using the universal joints to transmit power from the engine, encountered problems in the drive train. It was due to the rocking torques of the universal joints. Such torques were then analyzed by Dodge [16] and Evernden [17]. A comprehensive guide to the design of the universal joint was written by Wagner and Cooney [18]. The guide is about analyzing the kinematics and strength of the ideal universal joint without considering interference and assumes small joint angles. Hummel

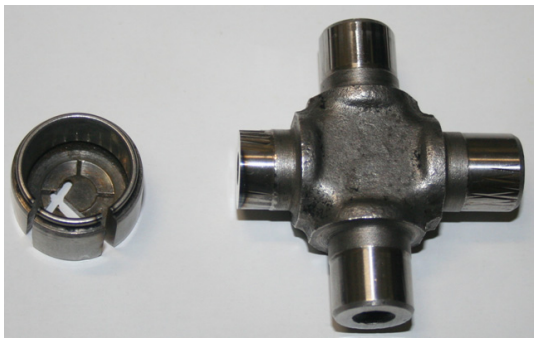

Fig. 3. Sample of a failed Cardan joint.

and Chassapis [14] investigated a systematic approach to the design and optimization of the ideal universal joint. It was shown that extremely high internal forces develop if contact occurs between the various components of the mechanism [19]. The high internal forces can cause failure; therefore, interference must be avoided at all times. Untimely joint failures were attributed to the rocking torque that was investigated by Dodge [16] and Evernden [17]. General universal joint design and dynamics guidelines have been written by Wagner and Cooney [18], Lee [20], Lingaiah [21], and Shigley and Mischke [22].

The need for advancing the power transmission mechanisms is endless. Engineers are restless in their attempts to explore more sophisticated systems that can do the job more efficiently. The need to transmit the power co-exists with the aspiration for reducing the levels of undesirable vibrations in the machineries. An example for such attempts can be found in the work reported by Chen, et al. [23]. They proposed a method for vibration isolation of a vertical axis through small amplitude of the suspension rod's axial force. By combing the geometric constraints and the governing dynamic equations they achieved a general governing equation for vibration isolation of the system.

In order to improve the quality of the power transmission systems, a second path is the improvement in the material content of the bearing surfaces. In can be performed in a way that advances the fatigue and the fracture resistance of the material while at the same time is friendlier to the environment. Sasaki [24] proposed surface modification for the bearings. Multi-Scale surface texturing that is a new concept of surface modification for tribo-materials, introduced as the expected future development. It is seen as an effective engineering technology that can contribute noticeably to sustainable societies.

Fig. 3 presents a failed Cardan joint bearing. The points of failure on the bearing are clearly marked in this figure. It is the focus of this research to investigate the causes of failure of these bearings and to propose some remedies for preventing such failures. It can consequently improve the bearing performance and increase its life-time.

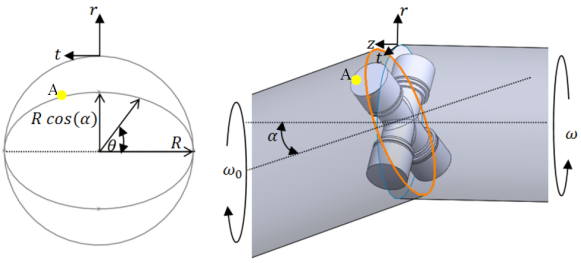

Fig. 4. An idealization of a Cardan joint.

3. Kinematics of the Cardan joint and the derivation of its motion equations

In order to accurately investigate the size of the oscillations in the output drive shaft and to calculate the maximum angular accelerations caused by the variations in the angular speed of the output drive shaft, one needs to resort to motion equations governing the Cardan joint [14, 25-27]. Such set of equations can be derived by using some geometrical relations between the selected points in a Cardan joint. Such is the one that is schematically presented in Fig. 4.

In Fig. 4, the locus of the points on the input and the output drive shafts are marked with two circles. In order to start with the derivations, consider a test point that is marked as point "A" on the output drive shaft. The distance from this point to the centre of the coordinate system "*r*", as a function of the angle of rotation of the output shaft "*θ*", can be calculated according to Eq. (1). This equation is based on the geometrical relations presented in Fig. 4.

$$r(\theta)=\sqrt{(R\ cos\theta)^2+(R\ cos\theta\ sin\theta)^2} \tag{1}$$

The velocity vector for the test point $\overrightarrow{V_A}$ is equal to

$$\overrightarrow{V_A}=\vec{V}_{A\bar{t}}+\vec{V}_{A\bar{z}} \tag{2}$$

where $\vec{V}_{A\bar{t}}$ and $\vec{V}_{A\bar{z}}$ are the tangential and normal components of the velocity at point "A", respectively.

$$\vec{V}_{A\bar{t}}=r(\theta)\times\omega \tag{3}$$

$$\vec{V}_{A\bar{z}}=\dot{z} \tag{4}$$

$$z=\sqrt{R^2-r(\theta)^2} \tag{5}$$

with θ = ωt, where "*z*" is the normal distance between point "A" and the output shaft, "*ω*" is the angular velocity of the input shaft and "*R*" is the shaft radius. It follows that

$$z=\sqrt{R^2-R^2\cos\omega t-R^2\cos^2\alpha\sin^2\omega t} \tag{6}$$

$$z=R\sin\omega t\sqrt{1-\cos^2\alpha} \tag{7}$$

$$\dot{z} = R\omega \times \sin\alpha \times \cos\omega t \tag{8}$$

$$\vec{V}_{A\bar{t}} = \omega R\sqrt{\cos^2\omega t + \cos^2\alpha \sin^2\omega t} \tag{9}$$

$$\vec{V}_{A\bar{t}} = \omega R\sqrt{1-\sin^2\alpha \sin^2\omega t}\ . \tag{10}$$

"α" is the deviation angle between the directions of the input and the output shafts. Substitution for $\vec{V}_{A\bar{t}}$ & $\vec{V}_{A\bar{z}}$ results in

$$\vec{V}_A = \sqrt{\vec{V}_{A\bar{t}}{}^2 + \vec{V}_{A\bar{z}}{}^2} = \omega R\sqrt{1-\sin^2\alpha \sin^2\omega t + \sin^2\alpha \cos^2\omega t}\ . \tag{11}$$

Eventually, one ends up with the following equations for the angular velocity "ω_o" and the angular acceleration "α_o" of the test point that is located on the Cardan joint output shaft

$$\omega_o = \frac{\vec{V}_A}{R} = \omega\sqrt{1+\sin^2\alpha \times \cos(2\omega t)} \tag{12}$$

$$\alpha_o = \frac{d\omega}{dt} = \frac{\omega^2 \sin^2\alpha \sin 2\omega t}{\sqrt{1+\sin^2\cos 2\omega t}}\ . \tag{13}$$

The above set of equations is merely based on the geometry of the Cardan joint. It is accurate and provides quick answers for the parameters of interest that are related to the joint. However, one may resort to engineering software that can produce the same sort of results at the expense of spending more time in model preparations. The later sections of this article rely on Solidworks in order to simulate some loading scenarios on the Cardan joint bearings. The geometry-based analytical method that is expanded in this section assists in verifying the preliminary results from the Solidworks modeling. It can provide an assurance that the numerical simulation stays in the right track and can provide reliable data. Therefore, the proposed analytical model and the simulation by the Solidworks in a sense have the task of confirming each other in consistency.

In order to observe oscillations in the angular speed, a Cardan joint with all details was modeled by using Solidworks engineering software [28]. Its input drive shaft was revolved at a constant angular speed equal to 36° per second. The corresponding results are presented in Fig. 5. It presents the variations in the angular speed of the output shaft of different inclination angles while the angular speed of the input shaft is kept constant.

Fig. 6 is a comparison between the output of the analytical results that are obtained by applying Eq. (12) and the results from modeling by the Solidworks software. The Solidworks modeling is needed to further analyze the Cardan joint. The input data to the two methods are the same and the results are in close agreement. While the analytical method produces exact results, there are slight differences of less that 0.01 percent between the peak values predicted by the two methods. This can be attributed to the inaccuracies inherent to the numerical modeling. This confirms the accuracy of the calculations and verifies the adequacy of the Solidworks modeling that is needed in the later sections of this research.

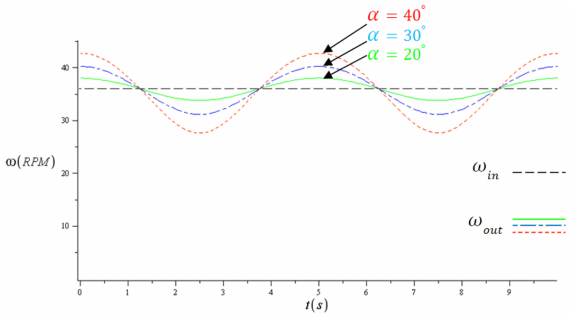

Fig. 5. The variations in the angular speed of the output drive shaft in Cardan joint of different inclination angles versus the angular displacement of the input drive shaft.

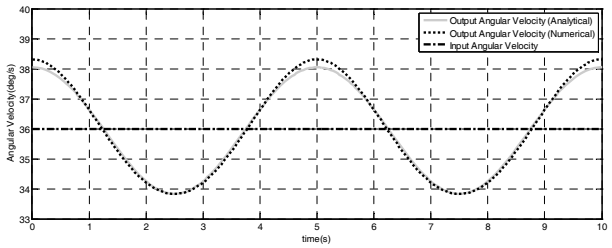

Fig. 6. The angular speed of the output drive shaft at the input drive shaft speed of 6 rpm. A comparison between the results from the Solidworks modeling and the analytical method.

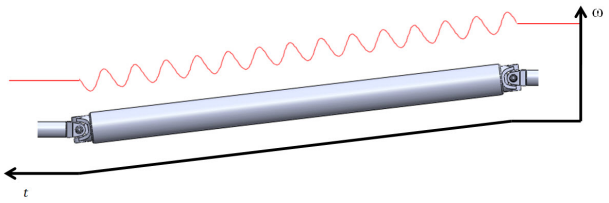

Fig. 7. The variations in the angular speed when using two successive Cardan joints.

It needs to be emphasized that the importance of the proposed analytical model is in the accuracy of its results.

It can be reliably used for the calculation of the maximum angular acceleration and the study of the parameters that influence the maximum moment of inertia. The same can be achieved through Solidworks modeling at the expense of spending time in model preparation and the loss of accuracy, to some extent.

A practical point in working with the Cardan joints is that by using a second joint that is fitted at the same angle on the subject shaft one can remove oscillations in the angular speed, altogether. This has been proved by expanding the analytical method also by the using the numerical solutions [29]. Very often, the simultaneous usage of two Cardan joints in mechanical systems is unavoidable. This removes the problem of oscillations in the angular speed that appears in the user component. This is schematically presented in Fig. 7.

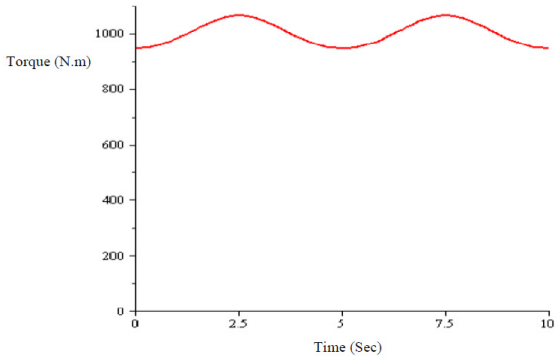

Fig. 8. The torque applied to the two ends of the shaft that connects the two consecutive Cardan joints (ignoring the system inertia).

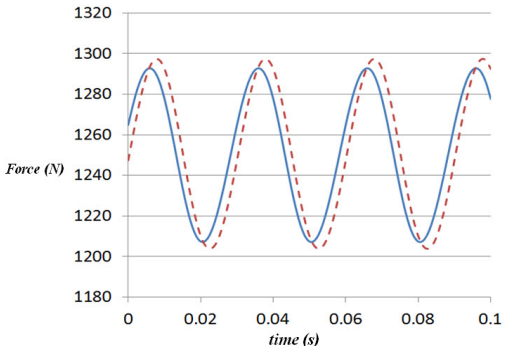

Fig. 9. Forces on the Cardan joint bearings with the shaft angle of 10°, the angular speed of 1000 rpm, and the transmitted torque of 100 N.m . The heavy line is for the bearing on the input shaft and the dashed line is for the bearing on the intermediate shaft.

4. Dynamic analysis and derivation of the bearing forces

The power transmitted by a rotating shaft can be calculated according to Eq. (14):

$$P = T\omega = cte \tag{14}$$

where "P" is the power transmitted, "T" is the transmitted torque and "ω" is the angular speed of the rotating shaft.

Also by considering the fact that the power input to the mechanism is constant and equal to its output power, one ends up with the following equation for the transmitted torque:

$$T_{out} = \frac{P}{\omega_{out}} = \frac{P}{\omega\sqrt{1+\sin^2\alpha\times\cos(2\omega t)}}. \tag{15}$$

As an example, based on Eq. (15), the calculated variations in the torque with the assumption of the angular speed of 6 rpm for the shaft and the transmitted power of 36 kW is presented in Fig. 8. It presents the oscillatory behavior of the torque that transmits through the intermediate shaft between the two Cardan joints. This is indeed verifying the existence of such oscillatory behavior.

The calculations for the exact value of the force and the size of the oscillations depend on the inertia of the intermediate shaft, inertia of the vehicle and variations in the torque arm in the Cardan joint mechanism. Such calculations are very difficult to be reached at. These forces are calculated numerically by using Solidworks engineering software [28]. The sample case is with the angular speed of 1000 rpm, resisting torque of 100 N.m and the shaft angle of 10°. As a result, the forces endured by the input drive shaft bearings and the intermediate shaft bearings are calculated and presented in Fig. 9.

It is clear from these results that the period for application of these forces are the same. It is resulted by the fact that the frequency of applying the force depends only on the angular speed of the input shaft. The phase differences between these forces also caused by the inertia of the components between the bearings.

The point to be noticed here is that the amplitude of force variations is higher for the bearing on the intermediate shaft compared to the input shaft bearing. This is attributed to the variations in the torque arm during revolving that increases the force amplitude. The important fact that can be deduced from Fig. 9 is that the possibility for the failure and damage to the bearings on the intermediate shaft is higher compared to the same type of bearings that are used on the input or the output shafts. The forces on the input shaft bearings are exactly proportional to the torque that is required to rotate the shaft. This indeed is the torque from the engine. Therefore, from this point on, all data are related to the engine torque instead of the force that acts on the bearings.

5. Analysis by using computer simulation and the calculation of the excess load

So far in this research, the oscillatory load on the Cardan joint bearings are identified and the causes of such oscillations are introduced. The oscillations that appear in the angular speed and the transmitted torque of the driven shaft consequently cause oscillations in the force and the resultant stresses in the bearings. Such effects are related to the geometry of the Cardan joint mechanism and are impossible to be removed. The question that comes into mind is about the effects of such oscillating forces on the Cardan joint bearings. Naturally, one may think of the failure and deformation of the bearing inner rings under such conditions. Fatigue failures are accompanied by the initiation and the spread of cracks and never cause deformation of the parts. Therefore, it is necessary to search for other causes for the Cardan joint bearing failures. In view of the fact that most reported deformations are caused by the impact loading [30], one needs to look for the presence of impact loading in these bearings. For the same reason and in order to study the forces that act on the Cardan joint bearings under overloading conditions, numerical simulation is used. The sample case is simulated by using the Solidworks engineering software in order to calculate the forces that act on the bearings. The following conditions are applied. The

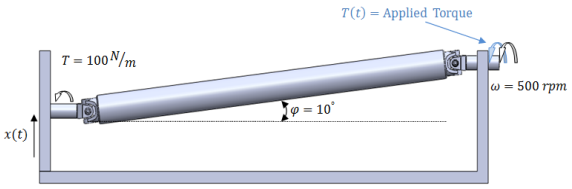

Fig.10. The setup for the numerical simulation of overloading a Cardan joint.

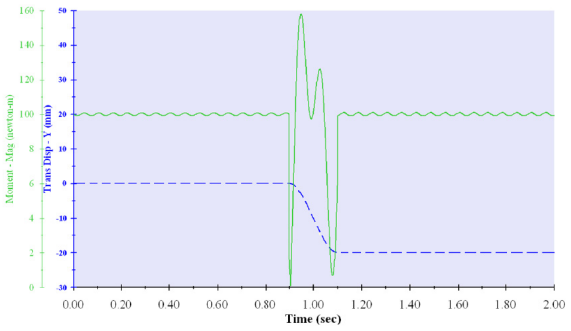

Fig. 11. Variations in the shaft vertical displacement (the dashed line) and the corresponding torque that is required for rotating the shaft at 500 rpm (the heavy line), "transmitted torque of 100 N.m".

input angular speed of the mechanism is 500 rpm and the shaft deviation angle is 10^{o}. The torque acting on the output shaft is 100 N.m. The downward displacement of 2 cm applied to the output shaft within 0.2 sec. Such conditions are presented in Fig. 10 and the results are presented in Fig. 11.

This numerical setup was to simulate the oscillations in the bearing forces while the output shaft tolerates displacement in the shape of a step of 2 cm in height. Such conditions are considered to be much softer than the real case scenarios. In reality, the forces acting on the bearings can be much higher. Nevertheless, in this case the maximum load happens to be 1.5 times the average load on the bearings. It is an indication of the sensitivity of the Cardan joint mechanism to the displacement of the output shaft. From the results that are presented in Fig. 11 and the working conditions of the system, presence of the multiple overloads in the system is unavoidable and the excessive amount of such overloading cannot be denied. Reaching at this important point in research, it becomes clear that the periodicity of the overloading is the main suspect for the deformation in the inner ring of the bearings. As presented in Fig. 11, the excess load has peak values that repeat periodically. Under the condition that the period of the excess loading peaks are independent of the output shaft displacement and only depend on the geometry of the mechanism, one can claim that such peaks appear at certain angular position in the surface of the bearing.

Concentration of the same excess loads at the same position that are caused by the repetitive nature of the loading, initiate the bearing deformation. To further study this issue, another numerical simulation was organized. This was to study the proportionality of the excess load peaks to other oscillatory

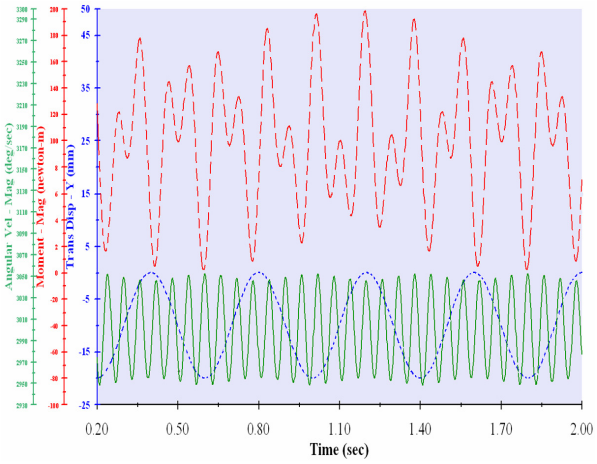

Fig. 12. The output shaft displacement (the dotted line), the angular speed of the intermediate shaft (the heavy line), the torque applied to the Cardan joint mechanism (the dashed line).

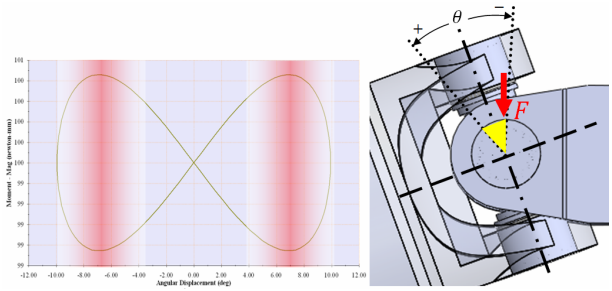

(a) (b)

Fig. 13. Results of a simulation of a Cardan joint under the condition that the output shaft carries a constant torque and the angular speed gradually increases from 10 to 100 rpm: (a) The torque that is required to drive the unit; (b) The zone on the inner ring of the bearing that endures the force (on the shaft that connects to the drive unit).

parameters that apply to the Cardan joint mechanism. This numerical setup resembles conditions of travelling over uneven road surfaces. In this case, the output shaft oscillations are at the frequency of 2.5 Hz with amplitude of 2 cm.

As a result, the torque required (that represents the forces acting on the bearing), the displacement of the output shaft and the angular speed of the intermediate shaft (that is proved to be oscillatory) are presented in Fig. 12. From such results, it is clear that the period for the excess loading does not depend on the displacement of the output shaft or on the environmental conditions. It depends only on the frequency of the variations in the angular speed of the intermediate shaft that is dependent on the angular speed input to the mechanism.

This is an indication of the fact that the excess loading applies only to some specific parts of the inner and the outer rings of the bearing. These exercises were continued in order to identify the parts of the inner and the outer rings of the bearing that bear the excess loads. In the third numerical simulation, no conditions are specified for the excess load. A constant resisting torque is applied to the end of the Cardan joint

Fig. 14. Samples of the failed Cardan joints that were examined for the purposes of this research.

mechanism and the angular speed input to the mechanism is gradually varied from 10 rpm to 100 rpm.

The corresponding output is presented in Fig. 13. From Fig. 13 and by considering the geometry of the subject Cardan joint it becomes clear that when the angle of the force transmission (ϕ in Fig. 10) is 10^{o}, only part of the inner ring (in a span of 20^{o}) endures the main force.

In addition, there are only a few numbers of the bearing needles that endure the loads. It also proves that the angular span for the maximum load acting on the bearing surface is not a function of the angular speed of the input drive shaft. In fact, such a span is a function of the geometry of the mechanism and it remains constant. This continues until the time the loaded zone deforms and the active area for the force shifts on the bearing surface. Another important point that is clear from Fig. 13 is the regular concentration of the points with maximum torque. Such points highlighted in Fig. 13(a) actually endure impact loads and lay at certain angular positions on the bearing surface.

6. Investigating the causes for the Cardan joint bearing failures

At this point in research, it is intended to investigate the causes for the deformation and damages endured by the bearing inner rings. Such an objective can be reached at by the proper examination of some failed Cardan joint bearings and also by careful study of the simulated results. It is also helpful to look back into the related documents that are already reported by the sophisticated bearing manufacturers.

It is intended to find some remedies for overcoming such bearing failures. In order to increase the accuracy of the results, 5 failed samples of the Cardan joints were selected. After some preparations, the damaged surfaces of those bearing samples were precisely examined. Fig. 14 presents a picture of the sets of the bearings that were used for the purposes of this research. The oscillatory nature of the forces endured by the bearings was identified and presented in section 4 of this article.

Moreover, the presence of the Hertzian stresses is a documented fact in contact mechanics and especially in the case of the sliding bearings. The results of the many studies indicate that the Hertzian stresses have their maximum amounts at the lower layers of the contact surfaces.

As a result of the presence of the maximum stresses such points are the most viable points for the movement of the dislocations and form their concentration points. Micro cracks start at such points and grow. The oscillatory natures of the forces that act on this specific bearing compel the cracks at the lower layers of the contact surface to grow faster and form larger cracks.

These cracks merge and cause separation of some small pieces of the material from the surface. Pitting in the surface is the sign of the presence of the Hertzian stresses. However, Hertzian stresses cannot be the only cause for the deformation in these bearings as such stresses are present in all bearings. When pitting happens, it reduces the surface of the inner ring that should endure the force. Consequently, this increases the surface stresses. The presence of the impact loading at such conditions causes large stresses that are higher than the yield stresses and the material enters into its plastic zone. The existence and the noticeable size of such impact forces already discussed in section 5. Since the depth and the surface of the section of the material that was separated by the Hertzian stresses are small, following the smallest plastic deformation the contact area of the balls and the inner ring increases and the material keeps on tolerating more stresses. Therefore, the reason for the deformations in this bearing is the presence of the impact loading in concert with the Hertzian stresses. This condition is already discussed in some references [30, 31]. Now there is the question that "why the presence of the impact loading does not cause such severe deformations in the other types of bearings?" As discussed in section 5 of this article, the answer is in the regularity of the impact loading in the case of the Cardan joint bearings. In fact, in other types of bearings as the bearing rotates all the balls endure the forces. Therefore, it is possible for the impact load to land on any balls at any moment. But in the case of the Cardan joint bearings, the impact load lands only on some specific balls at some specific angular span on the inner ring. In other words, after the impact loading causes the first deformation in the bearing, the Hertzain stresses and the oscillating load cause the crack initiation at the lower layers. This consequently causes pitting at some other parts of the inner ring. With the same trend as past, the impact load lands on the same point and forces the material to yield and to deform once more. It has to be emphasized that as a result of the geometrical specifications of this bearing configuration, the impact loads land repeatedly on the same point.

This practically causes some parts of the inner and the outer ring surfaces to stay safe from the impact loading while some other parts repeatedly suffer from the impact. Such processes are clearly visible in the microscopic pictures that were taken and are presented in Figs. 15 and 16. Since the contact surface of the needles with the inner ring surface is generally lower

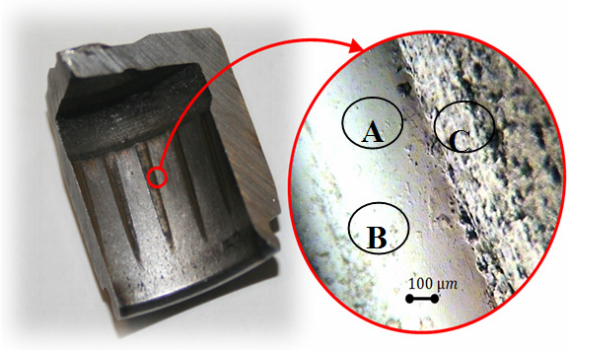

Fig. 15. Sample of the bearing outer ring and its microscopic image (magnification × 20): (A) The zone completely deformed by the impact loading; (B) The wear and crack re-growth at the deformed zone; (C) The zone without the impact loading and with higher rate of wear.

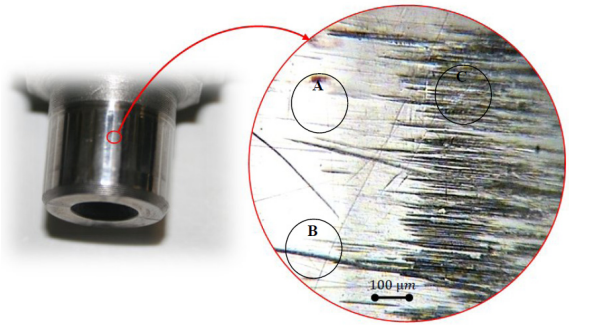

Fig. 16. Sample of the bearing inner ring and its microscopic image (magnification × 20): (A) The zone completely deformed by the impact loading; (B) The wear and the crack re-growth at the deformed zone; (C) The zone without the impact loading and with higher rate of wear.

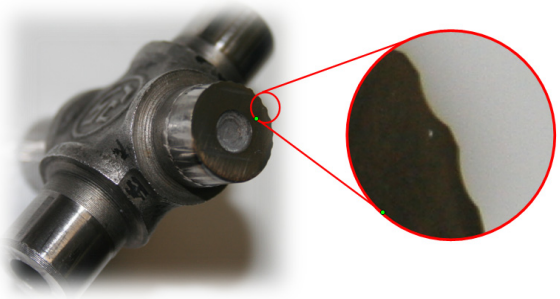

Fig. 17. The cross section of an inner ring of a Cardan joint bearing that is severely deformed.

than its contact with the outer ring surface, deformations at the inner ring surface are more severe. The impacts act on the ring surface by impacting the needles. As the time passes on and the Hertzian stresses continue, the process of the wear in the bearing surface continues.

The impact loads land on certain parts of the bearing and the needles gradually ditch and mark their effects on the ring surfaces. If the inner ring and the Cardan joint are manufactured as one piece, there are limits to its material stiffness. Practically and under the working conditions, the centre of the Cardan joint has to endure bending and the tension that follows. The stiff and brittle materials are very weak against fatigue and tensile stresses. With the assumption that the balls and the outer ring of the Cardan joint bearing are stiff enough, one can expect that the major damages happen at the inner ring of this bearing. Fig. 17 presents the surface of an inner ring that is severely deformed.

As a summary, the sequence of the events that are presented in Fig. 18 can be introduced as the main causes for the failure of the Cardan joint bearings.

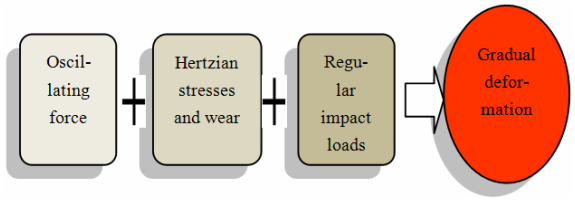

Fig. 18. The sequence of the events that end up to the deformation.

Fig. 19. Configuration of a Cardan joint with the intermediate spring and damper elements used in "ROA" automobiles.

7. Propositions for improving the life expectancy of the Cardan joint bearings

7.1 The use of the intermediate spring and damper to reduce the size of the impact loads

It is already stated in the last section of this article that the regular impact loading is the most effective cause for the deformation of the inner and the outer ring surfaces in the Cardan joint. As a first remedy, it is possible to remove the impact nature of the loading by installing a torsion spring and a damper in the middle of the Cardan shaft. This also omits the forces with large amplitudes. The effectiveness of this method is already discussed and reported in detail in the recent studies [32]. Fig. 19 presents an image for a two pieces Cardan shaft with the added intermediate spring and the damper.

Such configuration of the Cardan joint is used in the power transmission system of an automobile locally known with the brand name of "ROA". Such has been the configuration for the Cardan joint in ROA automobiles, since 2010. The team of ROA engineers believes that this set up has considerably reduced damage to the Cardan joint mechanism.

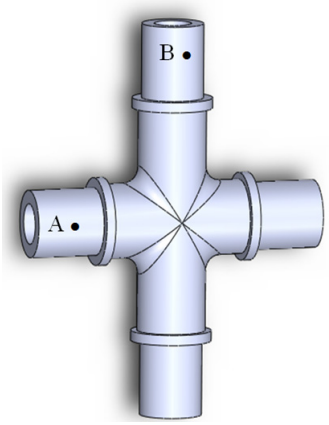

Fig. 20. A proposal for the Cardan joint with increased torque arm at the inner rings of the intermediate shaft bearings.

7.2 Reducing the load on the bearings that are viable to damage by increasing the torque arm

In section 4 of the article, it was stated that the force applied to the bearing on the intermediate shaft is higher than the load on the bearings on the input or the output shafts.

This is caused by the variations in the torque arm during the revolving of the shaft. It causes early damage to the Cardan joint bearings. The inner rings of the four bearings on the ends of the joint cross piece are manufactured as one piece. Consequently, when the time comes one has to replace the cross piece altogether. This happens while the bearings that connect to the outer shaft are not exposed to serious damages to the same extent as the bearings that connect to the intermediate shaft. Therefore, one may slightly increase the length of the arm of the Cardan joint that connects to the bearing on the intermediate shaft. This elongates the Cardan joint life span by allowing the four bearings to reach to their damaged status within the same time span.

Schematic design for such a bearing is presented in Fig. 20.

It needs to be reminded that the difference in the length of the arms of the Cardan joint depends on the operating angle of the joint. If the Cardan joint arms are out of proportion, this can increase the possibility for failure at the base. It is necessary to make sure that in practice the four bearings on the joint endure the same amount of maximum loading.

In order to examine the effectiveness of this proposal in lowering the loading on the Cardan joint cross piece arms, a numerical simulation by using Solidworks is arranged. The modeling conditions are the same as in Fig. 10. The input angular speed of the mechanism is 500 rpm and the shaft deviation angle is 10^{o}. The torque acting on the output shaft is 100 N.m. Two sample points on the Cardan joint cross piece are selected. In Fig. 20, these points are marked as point "A" on the shorter arm and point "B" on the longer arm. It is expected that the intermediate shaft should connect to the longer arm at point "B" and the input or the output drive shafts should connect to the shorter arm represented by point "A".

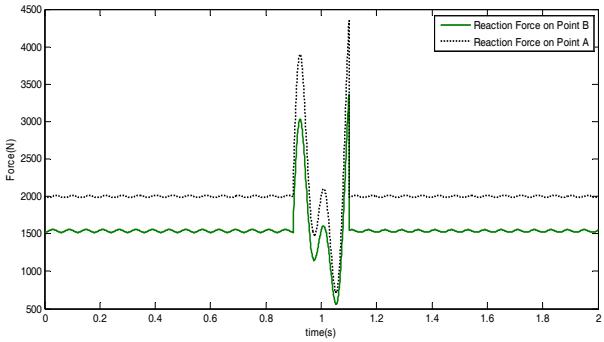

Fig. 21. Loading patterns for sample points "A" and "B" on the Cardan joint cross piece when the cross arm lengths are not equal (the results of simulation by using Solidwoks).

The results of the simulation in the form of the loading on the selected points are presented in Fig. 21. Clearly and as desired, the forces acting on point "B" that is located on the longer arm of the cross piece are lower than the forces acting on point "A". This is achieved by making the lengths of the cross piece arms unequal. Therefore, the bearings connecting to the intermediate shaft will no longer face with larger amount of loading compared to the bearings on the other ends of the cross piece.

It is possible to adjust the arm lengths to the sizes that will make the loadings on the bearings more manageable. Hence, it is concluded that this proposal is practical.

7.3 Increasing the degrees of freedom in order to remove the regularity in the impact loading

In section 5, it was stated that regularity in impact loading is amongst the most important factors in the deformation of the Cardan joint bearing inner rings. If one could remove the regularity in the impact loading, this certainly spreads the deformation throughout the ring surfaces. It can prevent emergence of the wavy appearance in the inner ring surface. In order to omit the regularity in the impact loading of the inner rings by the needle bearings, the idea of adding one degree of freedom to the bearing is proposed. It can be achieved by adding a second bearing to the system. The schematic of such configuration is presented in Fig. 22.

In such a bearing, the inner ring can revolve freely. This causes all the balls to enter into the angular zones of the forces that act upon them. Under such conditions all the balls will share the loads and endure the same amount of damage. Moreover, at the time of the impact, the contact point of the balls with the inner surface of the bearing will be randomly selected. Through such idea, surface of the inner ring will deform uniformly and the wavy appearance will not be formed. The idea of added roller bearings naturally increases the size and the price of the Cardan joint. However, it can be very useful for the special cases when the Cardan joint is hardly accessible or very costly to be replaced.

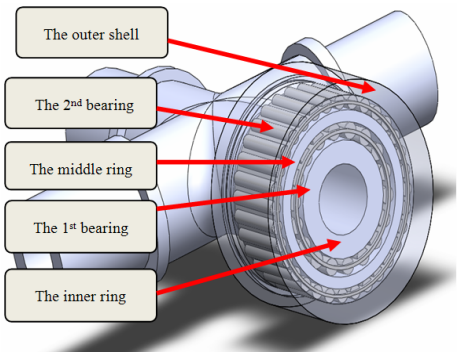

Fig. 22. A proposal for a Cardan joint equipped with two co-axial bearings in order to increase system degrees of freedom and to omit regularity in impact loading.

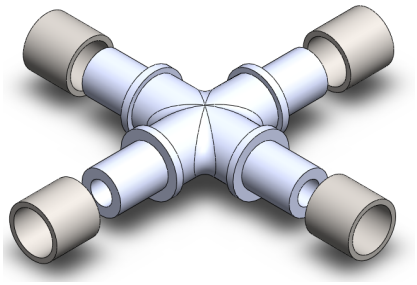

Fig. 23. A proposal for a Cardan joint equipped with 4 hardened rings.

7.4 Installing rigid rings over Cardan joint arms to act as the inner rings

Commonly, the Cardan joint and its' bearing inner rings are manufactured as one piece. This restricts rigidity of the inner rings. The brittle materials are very weak against tensile fatigue loads. The Cardan joint has bending load in its middle parts. This generates tension in its upper layers. Therefore, a proper recommendation can be the use of hardened metal bushes to act as the inner rings that sit on the four ends of the Cardan joint. This improves the performance of the inner rings without the need to alter the material content of the Cardan joint. A schematic of such a proposition is presented in Fig. 23.

8. Conclusions

The Cardan joint may appear as a simple component within a machine. It is no longer in use for many modern day automobiles. However, almost all semi heavy and heavy trucks and automobiles with engine power of more than 250 Hp have rear driving wheels and have to be equipped with Cardan joints. On the other hand, a Cardan joint is fairly cheap and very easy to be replaced. This can be performed during the routine maintenance services. But, it needs to be reminded that automobiles are not the only machineries that are equipped with Cardan joints. Other industries also use the Cardan joints in order to shift the direction or the alignment of the rotating shafts. Moreover, a damaged Cardan joint causes rigorous vibrations to its output shaft. Such vibrations can severely harm other components of the power transmission mechanisms. This certainly emphasizes on the importance of studying the Cardan joints and the parameters that can increase its performance and elongate its life time.

Therefore, the focal point in this research was to propose practical methods for increasing performance and the life expectancy of the Cardan joint bearings. It included studying the nature of the loads acting on the Cardan joint and its bearing surfaces. This was done analytically by considering the geometry and constraints of the Cardan joint.

A parallel task was the assessment of the Cardan joint behavior under loaded conditions through some numerical simulations.

Many damaged samples of the Cardan joints were also collected. The damaged sections of such joints were carefully examined. The analytical and the numerical simulated results were verified by comparing them with the outcome of the investigations about some damaged samples.

After careful examinations of the damaged bearings and by resorting to the analytical and the numerical simulated results some remedies are proposed. It is anticipated that such proposals can increase the performance and improve the life expectancy of the Cardan joints. These include:

- The use of the intermediate spring and damper to reduce the size of the impact loads
- Reducing the load on the bearings that are viable to damage by increasing the torque arm
- Increasing the degrees of freedom in order to remove the regularity in the impact load
- Installing rigid rings over Cardan joint arms to act as the inner rings.

With the aim of reducing damages to the Cardan joint and its bearings, one may choose a solution that is practically possible. It is also possible to combine some of the proposed methods to improve the quality of power transmission and to achieve a higher life expectancy for the bearings.

Further studies regarding the design, manufacturing processes and hardening of the Cardan joints can produce mechanisms that can perform more efficiently and last many folds, compared with the available devices.

Acknowledgements

The authors would like to acknowledge the support of the research office of Iran University of Science and Technology throughout the course of this study.

References

[1] I. I. Artobolevsky, *Mechanisms in modern engineering design*, (N. Weinstein, Trans.) Moscow: Mir Publisher, (1900).

[2] H. Hajirezaei and A. Ahmadi, Study on the effect of cracks in the failure of the Cardan joint, *The 6th international conference on maintenance*, Tehran (2010).

[3] H. Bayrakceken, S. Tasgetiren, and I. Yavuz, Two cases of failure in the power transmission system on vehicles: A universal joint yoke and a drive shaft, *International Journal of Engineering Failure Analysis*, 14 (4) (June 2007) 716-724.
[4] A. Covington, A universal idea, *Light & Medium Truck*, 28-29 (Jun. 2004).
[5] G. Erdman and G. N. Sandor, *Mechanism design*, Prentice Hall Publication (1991).
[6] A. Shirkhorshidian, *Design of mechanisms for designer and machine makers*, Nashretarrah Publication (2004) (in Persian).
[7] A. M. Heyes, Automotive component failures, *Engineering Failure Analysis,* 5 (2) (1998) 129-141.
[8] S. Tasgetiren, K. Aslantas and I. Ucun, Effect of press fitting pressure on the fatigue failure of spur gear tooth root, *Technol Res: EJMT* (2004) 21-29.
[9] Y. Ozmen, Tribological failures of machine elements and selection of suitable materials, *Technol Res: EJMT* (1) (2004) 31-37.
[10] C. Yuksel and A. Kahraman, Dynamic tooth loads of planetary gear sets having tooth Pro. Le wear, *Mechanism and Machine Theory*, 39 (2004) 695-715.
[11] V. R. Ranganath, G. Das, S. Tarafder and S. K. Das, Failure of a swing pinion shaft of a dragline, *Engineering Failure Analysis* (11) (2004) 599-604.
[12] H. Bayrakceken, Failure analysis of an automobile differential pinion shaft, *Engineering Failure Analysis*, 13 (8) (2006) 1422-1428.
[13] T. Kepceler, N. Tahrali and S. Eren, Stress analysis and life prediction of a 4.4 vehicles front and rear differential mechanism, *Automotive Technologies Congress*, Bursa, Turkey (2004).
[14] S. R. Hummel and C. Chassapis, Configuration design and optimization of universal joints with manufacturing tolerances, *Mechanism and Machine Theory*, 35 (2000) 463-476.
[15] S. R. Hummel and C. Chassapis, Configuration design and optimization of universal joint, *Mechanism and Machine Theory* , 33 (5) (1998) 479-490.
[16] A. Y. Dodge, *Automotive industries*, 1940.
[17] H. I. F. Evernden, The propeller shaft or hooke's coupling and the Cardan joint, *Proceedings of the Institute of Mechanical Engineers, Automotive Division*, 2 (1) (Jan. 1948) 100-110.
[18] E. R. Wagner and C. E. Cooney, Universal joint and driveshaft design manual, *Advances in Engineering Series*, No. 7, Society of Automotive Engineers, Warrendale, PA (1979).
[19] I. S. Fischer, Internal force and torque transmission in a Cardan joint with manufacturing tolerances, *Eng. Sci. D. Dissertation, Columbia University*, New York (1985).
[20] D. A. Lee, *Machine design* (1965).
[21] K. Lingaiah, *Machine design data handbook*, McGraw-Hill, New York (1994).
[22] J. E. Shigley and C. R. Mischke, *Standard handbook of machine design*, McGraw-Hill, New York (1986).
[23] H. W. Chen, W. X. Ji, Q. J. Zhang, Y. Cao and S. Y. Fan, A method for vibration isolation of a vertical axis automatic washing machine with a hydraulic balancer, *The Journal of Mechanical Science and Technology*, 26 (2) (2012) 335-343.
[24] S. Sasaki, Environmentally friendly tribology (Eco-tribology), *The Journal of Mechanical Science and Technology*, 24 (1) (2010) 67-71.
[25] S. F. Asokanthan and P. A. Meehan, Non-linear vibration of a torsional system driven by Hooke's joint, *Journal of Sound and Vibration* (2000) 297-310.
[26] S. I. Chang, Torsional instabilities and non-linear oscillation of a system incoporating a Hooke's joint, *Journal of Sound and Vibration* (2000) 993-1002.
[27] V. Zeman, Dynamik der drehsysteme mit kardangelenken, *Mechanism and Machine Theory*, 13 (1977) 107-118.
[28] S. Dassalt, *Solidworks documentation*, Jan. 2009.
[29] J. Eddie Baker, Displacement-closure equations of the unspecialised double-Hooke's-joint linkage, *Mechanism and Machine Theory* (March 5, 2002) 1129-1140.
[30] P. I. SKF, *Bearing failures and their causes*, Sweden: Palmeblads Tryckeri (2004).
[31] TIMKEN, *Tapered roller bearing damage analysis*, USA: Timken Company (2003).
[32] M. Browne and A. Palazzolo, Super harmonic nonlinear lateral vibrations of a segmented driveline incorporating a tuned damper excited by non-constant velocity joints, *Journal of Sound and Vibration*, 323 (1-2) (June 2009) 334-351.

Farzad Vesali was born in 1987. He holds a bachelor degree in mechanical engineering from Bu-Ali Sina University in Hamedan, Iran. He is currently a post-graduate student at the School of Railway Engineering at Iran University of Science and Technology in Tehran. Farzad is interested in the bearings and the dynamics of the rotating machineries. He is also actively involved with the industry regarding the vibration analysis and the maintenance of industrial machineries.

Mohammad Ali Rezvani, born in 1960, holds his Ph.D in mechanical engineering. He graduated from the University of New South Wales in Sydney Australia, in 1995. Dr. Rezvani is an academic at the School of Railway Engineering at Iran University of Science and Technology. His areas of expertise include wear and tribology, modal analysis and mechanical system design. Dr. Rezvani is also the head of the advanced vibration laboratory at the School of Railway Engineering. The laboratory provides services for the Modal testing of the railway infrastructure and railway rolling stocks. Dr. Rezvani is a member of the national committee for the condition monitoring and fault diagnosis of machineries, in Iran.